Int. J. Electrochem. Sci., 17 **(2022)** Article Number: 220250, doi: 10.20964/2022.02.44

International Journal of
ELECTROCHEMICAL
SCIENCE
www.electrochemsci.org

Synthesis of Ru(IV) modified Pt/C electrocatalyst and its application for enhanced methanol electrooxidation

Shaojun Li, Junming Chen and Lei Bai**

College of Chemistry and Materials Engineering, Anhui Science and Technology University, Bengbu, Anhui, China, 233030
*E-mail: cjmmap@163.com, baileiwj2014@163.com

Received: 30 Octeober 2021 / *Accepted:* 13 December 2021 / *Published:* 5 January 2022

Commercial Pt/C was modified with Ru (IV) species via the hydrolysis of Ruthenium (III) nitrosyl nitrate under a hydrothermal condition. It was revealed that the Pt nanoparticles were surrounded by Ru (IV) species and the presence of Ru (IV) species modified the electronic structure, which lowed the binding energy of Pt atoms. The results from the methanol electrooxidation suggested that the current intensity was increased and at the same time, the onset potential was decreased largely in the presence of Ru(IV) species modified Pt/C, which demonstrated the fact that the Ru (IV) species could activate the water molecules to provide the OH* to remove the CO_{ads} at low potential.

Keywords: Commercial Pt/C; Ru (IV) species; chemical modification; catalytic electrooxidation

1. INTRODUCTION

Platinum (Pt) based nanomaterials have been well demonstrated to be the most efficient catalysts for the energy conversion, such as the direct methanol fuel cell. [1–3] However, the high cost and low availability limits the application to a large extent. In order to enhance the catalytic activity of Pt nanomaterials, several methods had been developed such as the synthesis of Pt alloyed catalysts with 3d transition metals, which generally have controllable shapes and compositions, as well as the modification of the supports for the Pt nanomaterials.[4–10] Meanwhile, the possible mechanism concerning the methanol electrooxidation over Pt based alloys was also proposed.[11] The bifunctional mechanism indicated that the coexisted other components adjacent to Pt species could provide the oxygen species produced to oxidize the poisoning intermediates [$(CO)_{ads}$]. The other mechanism known as the electronic effect proposed that the coexisted component could modify the electronic properties of Pt atoms, which both decreased the $(CO)_{ads}$ bonding energy and increased the $(CO)_{ads}$ tolerance.[12,13]

It is worth mentioning that generally, the commercial Pt/C always was used as the reference in the methanol electrocatalyitc oxidation to evidence the advantages of the new synthesized Pt based alloys.[14–16] As for the Pt/C powders, due to the fact that they are commercial sample, the effort to enhance their electrocatalytic performances seems to be rare and thus, it could be interesting to explore the possibility for promoting the activity of the commercial samples. Accordingly, in this work, we employed the hydrothermal method to deposit the Ru species on the commercial Pt/C by using Ruthenium nitrosyl nitrate and the results from the methanol electrooxidation suggested that on the one hand, the mass and specific activity of the Ru modified Pt/C could achieve up to 1.8 and 2 -fold higher than those of commercial Pt/C. More importantly, the onset potential of the methanol electrooxidation over the Ru modified Pt/C was shifted more than 150 mV (vs SCE) compared with Pt/C. Besides, it was confirmed that the above treatment could be applied for the commercial Pd/C to increase electrooxidation of formic acid. It is expected that the present work would provide some new insights for the surface modification and the improving the performances of the commercial electrocatalysts.

2. EXPERIMENTAL

All the reagents were analytical pure and used without further treatment. Commercial Pt/C (Pt, 20 wt.%) and Ruthenium nitrosyl nitrate solution [$Ru(NO)(NO_3)_3$, Ru 1.5% w/v] was purchased from Sigma-Aldrich and Aladdin, respectively.

10 mg Pt/C with 50 μL or 100 μL $Ru(NO)(NO_3)_3$ was added into 10 mL distilled water and sonicated for 30 min to obtain a homogeneous solution, respectively. Then, the solutions were transferred into a 25 mL Teflon-lined stainless-steel autoclave and heated at 443 K for 3 h. After cooling to room temperature, the samples were collected and washed by ethanol-acetone (V:V= 1:1) for 3 times and finally, dried at 313 K overnight for further use. The two samples were named as Pt/C-Ru-50 and Pt/C-Ru-100, respectively.

Finally, 4 mg of the Pt/C, Pt/C-Ru-50 and Pt/C-Ru-100 were dispersed into the mixed solution containing 0.98 mL DMF and 0.02 mL Nafion (5%), respectively. After ultrasonic treatment for a certain time, 10 μL of the ink was loaded on a polished glassy carbon electrode with 3 mm in diameter and used after drying naturally.

3. RESULTS AND DISCUSSION

The XRD patterns of Pt/C before and after modifying by Ru(IV) were shown in Fig.1. As indicated the patterns, the peaks at 39.9, 46.4 and 67.7^o were ascribed to the (111), (200) and (220) crystal planes of metallic Pt, respectively. Besides, the peak at 25.4^o was due to the carbon. Clearly, before and after modification, no shift of the peaks of Pt was noticed, suggesting that the processing did not lead to the formation of alloys of Pt and Ru. It was worth mentioning that no peaks due to Ru(IV) were observed on the patterns, which was possibly due to the small size or poor crystallinity.

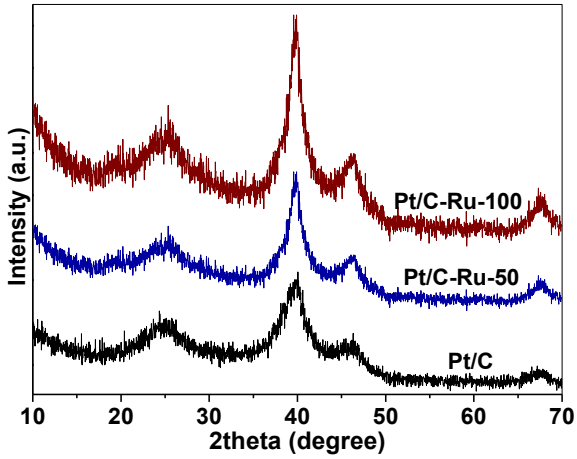

Figure 1. XRD patterns of Pt/C, Pt/C-Ru-50 and Pt/C-Ru-100.

Furthermore, the TEM and HRTEM images of Pt/C were shown in SFig.1. As displayed in SFig.1A, the fine Pt nanoparticles were nearly dispersed on the carbon and the average distance of 0.225 nm was ascribed to the (111) crystal plane of Pt as evidenced by SFig.1B.

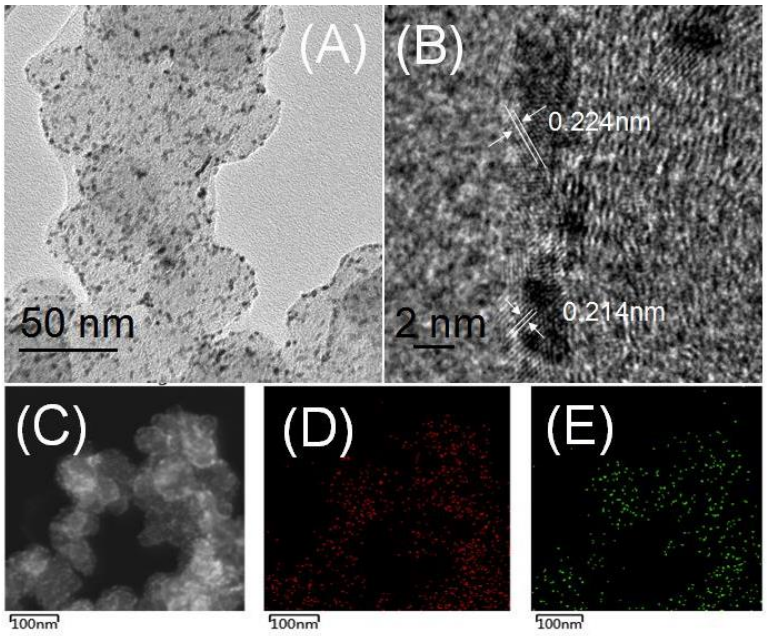

Figure 2. TEM (A), HRTEM (B), HADDF-STM image (C) and EDX element distribution of Pt (D) as well as Ru (E) of Pt/C-Ru-50.

After introducing of Ru species, the fine particles were not changed as indicated by the TEM image in Fig.2A. Additionally, the HRTEM image in Fig.2B displayed the average distance of 0.224 and 0.214 nm could be ascribed to the (111) crystal plane of Pt as well as (210) crystal plane of RuO_2. From the HADDF-STEM and elemental mapping from Fig.2C to E, it was suggested that the Ru species were

heterogeneously dispersed on the Pt/C. The relative contents of Pt and Ru were calculated in STable 1.

In order to know the chemical state of the elements, XPS analysis was performed for the samples. As displayed in Fig.3A, the peaks at 71.8, 75.1 eV and 72.7, 75.8 eV were ascribed to the metallic Pt and Pt oxides, respectively. After introduction of Ru species, these peaks shifted to 71.2, 74.5 eV and 72.3, 75.5 eV for both Pt/C-Ru-50 and Pt/C-Ru-100, respectively. From this information, it was indicated that on the one hand, before and after introduction of Ru species, the state of Pt in the samples were generally in metallic state and slight oxides were found on the surface as well as on the other hand, the binding energy of the metallic Pt shifted to a lower value after modification with Ru species.[17] The shift could be due to the electrons transferring from Ru (IV) species to the Pt atoms. These observations indicated the charge transfer from Ru (IV) species to Pt and led to the lowering of the d-band energy of Pt. As reported in the previous work, the lower d-band energy was generally associated with weaker adsorbate binding on the surface of metal, which was favorable for improving the catalyst activity. [18,19] Furthermore, the XPS spectra of Ru 3p 3/2 in Pt/C-Ru-50 and Pt/C-Ru-100 were present in Fig.3B. The peaks centered at 463.1 eV were ascribed to the existence of Ru (IV) species [20] and this results suggested that the $Ru(NO)(NO_3)_3$ was oxidized and hydrolyzed under the present hydrothermal condition.[21,22]

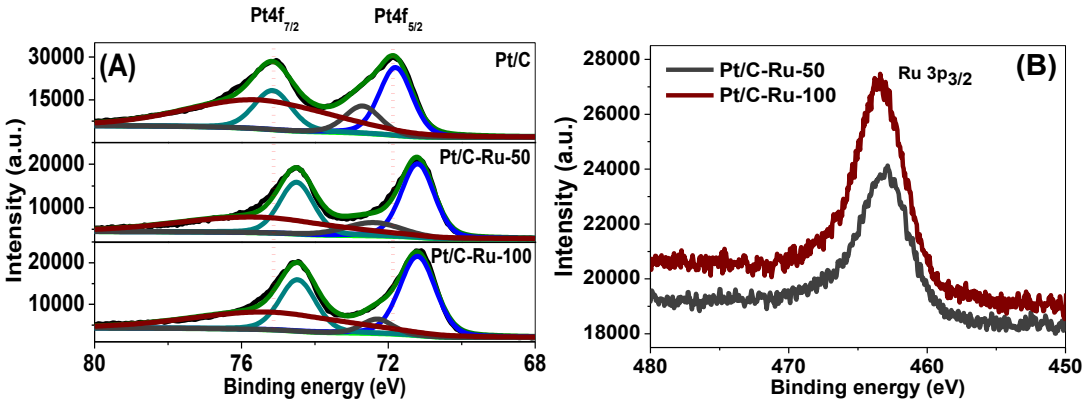

Figure 3. XPS spectra of Pt 4f (A) and Ru 3p (B)

The electrochemically active surface areas (ECSA) were calculated to be 31.0, 34.1 and 33.4 m2/g Pt based on the CV in SFig.2. The CV curves of the methanol oxidation of Ru (IV) modified and raw Pt/C after Pt mass-normalization were shown in Fig.4A. It was suggested that the activity of the electrocatalyst was generally evaluated by the current intensity and onset potential. On the one hand, the onset potential of the methanol oxidation was about 0.03 V for both Pt/C-Ru-50 and 100 compared with 0.187 V for Pt/C, indicating that a large decrease of the onset potential was achieved. On the other hand, as displayed in Fig.4B, the values of the mass activity were 375, 345 and 206 mA/mg Pt for Pt/C-Ru-50, Pt/C-Ru-100 and Pt/C, respectively and in addition, the specific activity was as following: Pt/C-Ru-50 (1.21 mA/cm^2), Pt/C-Ru-100 (1.01 mA/ cm^2) and Pt/C (0.62 mA/ cm^2). Thus, 1.8 and 1.95-fold higher in the mass and specific activity after modification was observed. The ratios of the first anodic peak (I_f)/ the backward anodic peak (I_b) were calculated to illustrate the anti-poisoning ability and these values

were 1.11, 1.35 and 0.93 for Pt/C-Ru-50, Pt/C-Ru-100 and Pt/C, respectively, which indicated that the Ru (IV) modified Pt/C had a better anti-poisoning ability. In the following, Chronoamperometry was employed to investigate the electrochemical activity and stability of these samples after the stable CV curves of methanol electrooxidation were obtained. The changes of the current intensity in the presence of Pt/C-Ru-50, Pt/C-Ru-100 and Pt/C in 1200 s were displayed in Fig. 4C. Clearly, the current density of the Pt/C-Ru-50 was much higher (63.5 mA/mg Pt) than those of Pt/C-Ru-100 (29.4 mA/mg Pt) and Pt/C (11.8 mA/mg Pt), further evidencing the promoting effect of the Ru(IV) in the commercial Pt/C. Finally, the electrochemical impedance spectroscopy (EIS) was carried out and the Nyquist plots were displayed in Fig. 5D. It was observed that the diameters of impedance arc (DIAs) decreased in such an order: Pt/C > Pt/C-Ru-100 > Pt/C-Ru-50. According to the previous work, the results suggested that the Pt/C-Ru-50 had a lower charge transfer resistance, which implied that a quick charge transfer rate could be realized between the catalyst and methanol molecules and a better catalytic performance was observed. [14,16]

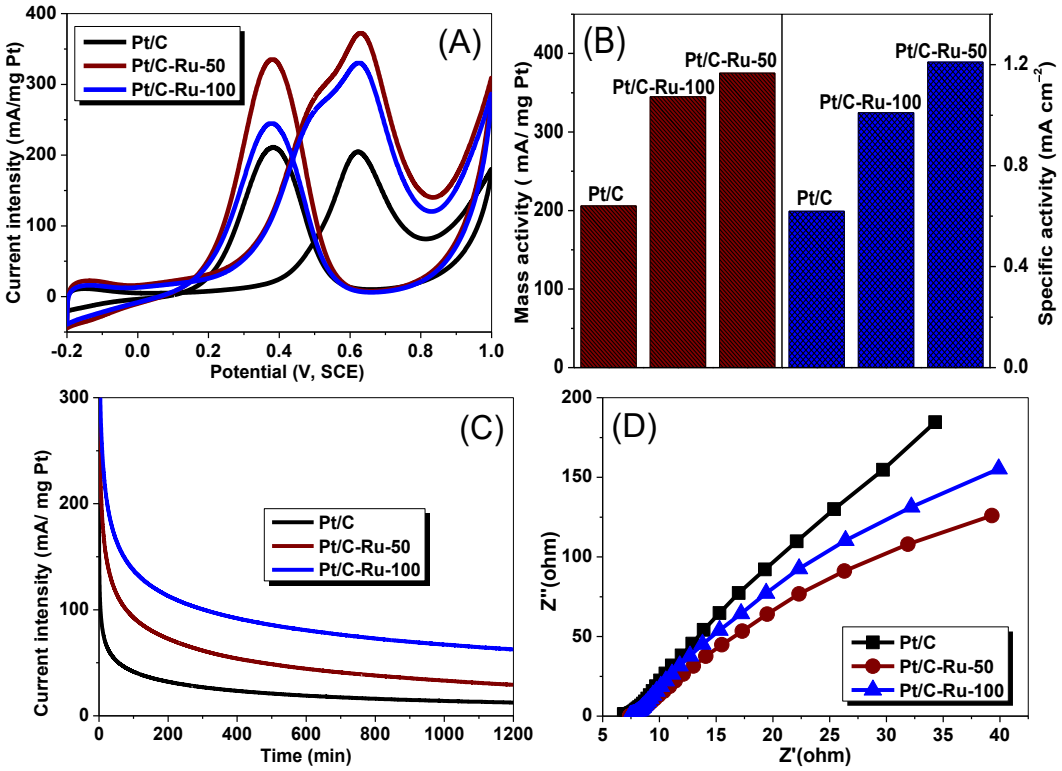

Figure 4. (A) CV curves of methanol oxidation in 0.5 M H_2SO_4 + 1.0 M CH_3OH solution at a sweep rate of 50 mV·s $^{-1}$. (B) Comparison of mass (brown) and specific activity (blue). (C) Current-time curves recorded at 0.65 V. (D) EIS Nyquist plots of methanol electrooxidation in 0.5 M H_2SO_4 + 1.0 M CH_3OH solution at 0.4 V with Pt/C-Ru-50, Pt/C-Ru-100 and Pt/C.

There are two mechanisms concerning the explanation of the methanol electrooxidation in the presence of Pt based catalysts, which are called as The bi-functional mechanism and the electronic effect.[11, 17] The mechanism can be described by the following Equations from 1 and 2:

$Pt—(CH_3OH)_{ads} \rightarrow Pt\text{-}CO_{ads} + 4\ H^+ + 4\ e^-$ (1)

$CO_{ad}–Pt + Pt + H_2O \rightarrow CO_{ad}–Pt + OH_{ad}–Pt + H^+ + e^- \rightarrow 2Pt + CO_2 + 2\ H^+ + 2\ e^-$ (2)

$Pt—(CH_3OH)_{ads} \rightarrow Pt\text{-}CO_{ads} + 4\ H^+ + 4\ e^-$ (3)

$CO_{ad}–Pt + Ru(IV) + H_2O \rightarrow CO_{ad}–Pt + OH_{ad}–Ru(IV) + H^+ + e^- \rightarrow Pt + Ru(IV) + CO_2 + 2\ H^+ + 2\ e^-$ (4)

After the modification of Ru(IV), the mechanism could be slightly changed as described by Equations from 3 and 4, which suggested that the enhanced performances of the methanol electrooxidation were possibly ascribed to the increased ability of removal of poisoning intermediates.

Finally, on the one hand, for evidencing the repeatability of the present strategy, the different batch of the Pt/C-Ru-50 was prepared and tested for the methanol electrooxidation and as shown in SFig.3, only a very slight difference was noticed, which suggested a good repeatability of this synthetic strategy.

4. CONCLUSION

Ru (IV) species modified commercial Pt/C catalyst was achieved by the hydrothermal method. The results from the structure analysis suggested that a part of Pt nanoparticles on the Pt/C were surrounded by the Ru (IV) species originated from $Ru(NO)(NO_3)_3$ and the presence of Ru (IV) species modified the electronic structure of the Pt atoms. The data in the catalytic tests suggested that on the one hand, the appropriate amount of Ru(IV) species modified Pt/C not only shown an enhanced current intensity, but also a large decrease of onset potential in the methanol electrooxidation compared the raw Pt/C, which was possibly due to the promoting effect of Ru (IV) species. It was believed that this work could provide a new insight for chemical modification of commercial electrocatalysts with enhanced performances for the energy conversion application.

ACKNOWLEDGMENT
This work is supported by the Domestic Visiting Scholar Program for Outstanding Young Talents of Anhui Province (No. gxgnfx2021135). The Talent Introduction Project of Anhui Science and Technology University (NO.830166) and 2019 were appreciated for financial support.

SUPPORTING INFORMATION:

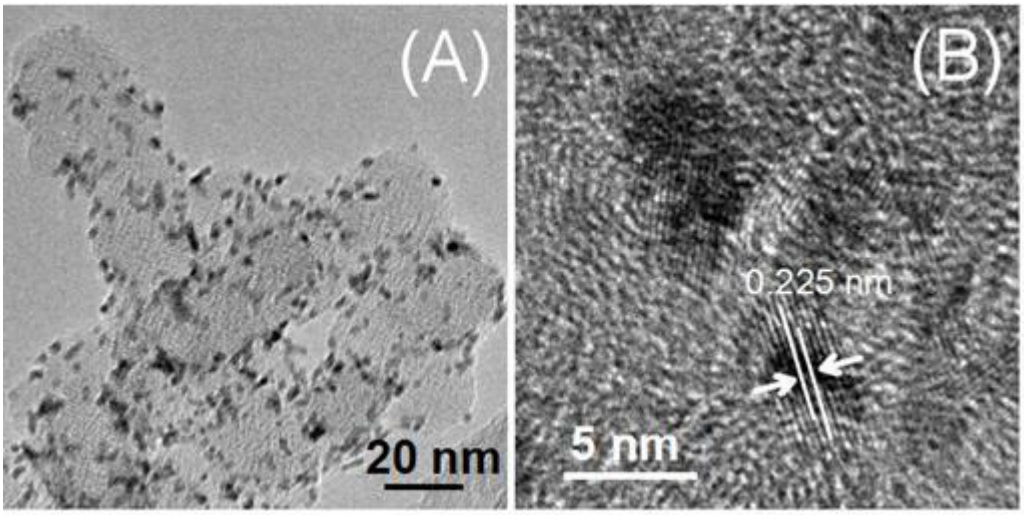

SFig. 1 TEM (A) and HRTEM (B) images of commercial Pt/C.

STable 1. EDX results of the weight ratio of Pt and Ru.

Sample	Pt/Ru
Pt/C	/
Pt/C-Ru-50	72.8/22.2
Pt/C-Ru-100	62.5/37.5

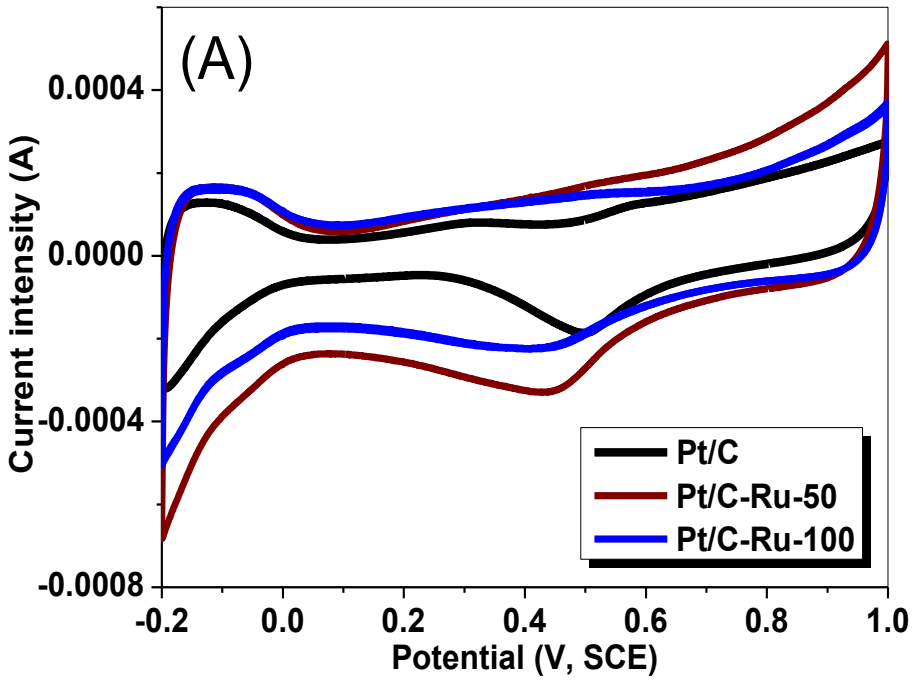

SFig. 2. CV curves in 0.5 M H_2SO_4 at a sweep rate of 50 $mV \cdot s^{-1}$ for the catalysts.

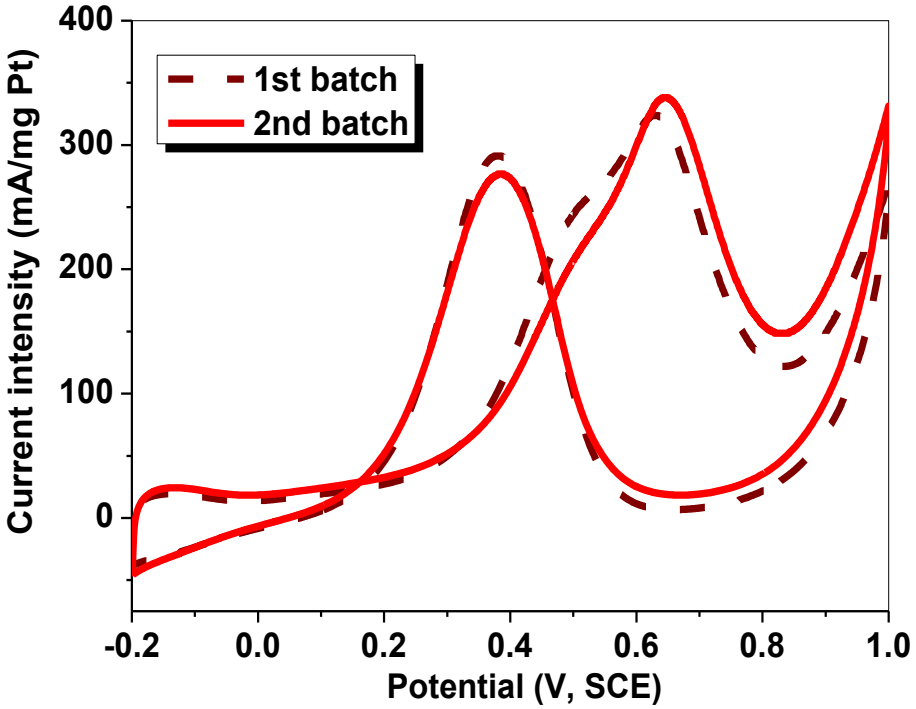

SFig. 3. CV curves of methanol oxidation in 0.5 M H_2SO_4 + 1.0 M CH_3OH solution at a sweep rate of 50 $mV \cdot s^{-1}$ for two different batches.

References

1. L.Y. Gong, Z.Y. Yang, K. Li, J.J. Ge, C.P. Liu and W. Xing, *J. Energy Chem.*, 27 (2018) 1618.
2. N. Kakati, J. Maiti, S.H. Lee, S.H. Jee, B. Viswanathan and Y.S. Yoon, *Chem. Rev.*, 114 (2014) 12397.
3. X.Y. Huang, A.J. Wang, X.F. Zhang, L. Zhang and J.J. Feng, *ACS Appl. Energy Mater.*, 1 (2018) 5779.
4. Z.R. Li, Z.Y. Guan, Y.T. Chang, D. Hu, B.K. Jin and L. Bai, *CrystEngComm*., 22 (**2020**) 1442.
5. Y.Y. Zhang, R. Shi, J. Ren, Y. Dai, Y.J. Yuan and Z.H. Wang, *Langmuir*, 51 (2019) 16752.
6. X.L. Tian, L.J. Wang, P.L. Deng, Y. Chen and B.Y. Xia, *J. Energy Chem*., 26 (2017) 1067.
7. X. Li, Y. Lv and D. Pan, *Colloid Surf. A: Physicochem. Eng. Asp.*, 569 (2019) 110.
8. L. Bai and Y.W. Bai, *J. Nanopart. Res*., 20 (2018) 24.
9. C.S. Shang, Y.X. Guo and E.K. Wang, *Nano Res.*, 11 (2018) 6375–6383.
10. X. Q. Wang, M.L. Sun, S. Xiang, M. Waqas, Y.J. Fan, J.P. Zhong, K.X. Huang, W. Chen, L.J. Liu and J. Yang, *Electrochim. Acta*, 337 (2020) 135742
11. D.J. Chen and Y.Y.J. Tong, *Angew. Chem.-Int. Edit.*, 54 (2015) 9394.
12. L. Bai, *Dalton Trans*., 45 (2016) 4712.
13. Sugimoto, K. Aoyama, T. Kawaguchi, Y. Murakami and Y. Takasu, *J. Electroanalytical Chem.*, 576 (2005) 215.
14. S.L. Lu, K. Eid, D.H. Ge, J. Guo, L. Wang, H.J. Wang and H.W. Gu, *Nanoscale*, 9 (2017) 1033.
15. C.Z. Li, T.Y. Liu, T. He, B. Ni, Q. Yuan and X. Wang, *Nanoscale*, 10 (2018) 4670.
16. J.Y. Liu, G.R. Xu, B.C. Liu and J. Zhang, *Chem. Commun.*, 53 (2017) 7457.
17. L. Bai, S.J. Li, L. Fang, Z.P. Chen and Z.R. Li, *Langmuir*, 36 (2020) 7602.
18. K. Guo, Y. Liu, M. Han, D.D. Xu and J.C. Bao, *Chem. Commun.*, 55 (2019) 11131.
19. G. Wu, L. Li, J.-H. Li and B.-Q. Xu, *J. Power Sour*., 155 (2006) 118.

20. F. Pan, J. Yang, J. Cai and L Liu, Res. *Chem. Intermediat.*, 47 (2021) 4595.
21. M. Ristić, M. Marciuš, Ž. Petrović, M. Ivanda, S. Musić, Mater. Lett., 156 (2015) 142.
22. S.-Y. Chen, M. Nishi, A. Chang, W.-C. Hsiao, T. Mochizuki, H. Takagia and C.M. Yang, *Sustain. Energy Fuels*, 4 (2020) 5802.